Shoot nitrate status regulates Arabidopsis shoot growth and systemic transcriptional responses via shoot adenylate isopentenyltransferase 3

Kota Monden[a†], Takamasa Suzuki[b], Mikiko Kojima[c], Yumiko Takebayashi[c], Daisuke Sugiura[d], Tsuyoshi Nakagawa[a], Hitoshi Sakakibara[c,d], and Takushi Hachiya[a†]

[a]Department of Molecular and Functional Genomics, Interdisciplinary Center for Science Research, Shimane University, 1060 Nishikawatsu-cho, Matsue, Shimane 690-8504, Japan

[b]College of Bioscience and Biotechnology, Chubu University, 1200 Matsumoto-cho, Kasugai, Aichi 487-8501, Japan

[c]RIKEN Center for Sustainable Resource Science, 1-7-22 Suehiro-cho, Tsurumi-ku, Yokohama, Kanagawa 230-0045, Japan

[d]Graduate School of Bioagricultural Sciences, Nagoya University, Furo-cho, Chikusa-ku, Nagoya, Aichi 464-8601, Japan

[†]Corresponding authors

Corresponding authors:

Kota Monden (n23d203@matsu.shimane-u.ac.jp)

Takushi Hachiya (takushi.hachiya@life.shimane-u.ac.jp)

Funding:

This study was supported by JSPS KAKENHI [No. 20K05771 and 23K04978 to TH and No. JP24KJ1709 to KM], by JST SPRING [No. JPMJSP2155 to KM], and by the Sasakawa Scientific Research Grant from the Japan Science Society [No. 2022-4039 to KM].

Keywords:

Arabidopsis thaliana; cytokinin; IPT3; isopentenyltransferase; micrografting; NR; nitrate reductase; nitrate signal; nitrate accumulation; systemic regulation

Abstract

Plants systemically regulate growth and gene expression according to their internal nitrate status. Our previous study reported that shoot nitrate accumulation increases shoot expression of adenylate *ISOPENTENYLTRANSFERASE 3* (*IPT3*) and shoot levels of N^6-(Δ^2-isopentenyl) adenine (iP)-type cytokinins (CKs). *IPT3* expression is localized in the phloem, and iP-type CKs, which are synthesized by IPT3, are phloem-mobile. As CKs are a class of phytohormones that control growth and genome-wide gene expression, shoot-expressed IPT3 may mediate the systemic regulation of growth and transcriptomic responses to shoot nitrate status. To examine this, we developed a novel system to manipulate nitrate levels and *IPT3* expression in a shoot-specific manner and performed growth analysis, CK determination, and RNA-sequencing. Our results demonstrated that shoot nitrate accumulation significantly promoted shoot growth and elevated shoot concentrations of iP ribotides, iP-7-*N*-glucoside, and iP-9-*N*-glucoside through the action of shoot IPT3. Transcriptomic responses to shoot nitrate accumulation were largely tuned by shoot IPT3, with opposite effects in shoots and roots. Shoot IPT3 amplified shoot responses of nitrate-inducible genes and immune response genes to shoot nitrate accumulation, while dampened root responses of nitrate transport/assimilation genes. This transcriptomic modulation via shoot IPT3 was accompanied by coherent transcriptional changes in genes encoding mobile peptides and transcriptional repressors. Here we present a novel scheme integrating shoot nitrate status responses with CK signaling.

Introduction

Land plants use soil nitrate and ammonium as primary nitrogen sources (Hachiya and Sakakibara 2017). Root-absorbed nitrate is reduced to ammonium via the sequential actions of nitrate reductase (NR) and nitrite reductase (NiR). Ammonium, whether taken up by the roots or generated through nitrate reduction, is assimilated into Gln and Glu by the enzymes glutamine synthetase (GS) and glutamate synthase (GOGAT). These amino acids serve as precursors for the

53 biosynthesis of other amino acids. Nitrate serves as a building block for organic nitrogen
54 biosynthesis and as a signaling molecule (Remans et al. 2006; Wang et al. 2004). The addition of
55 exogenous nitrate to nitrate-depleted plants rapidly changes the expression of nitrate-responsive
56 genes, a phenomenon termed as the primary nitrate response (PNR) (Medici and Krouk 2014). In
57 *Arabidopsis*, the nitrate transceptor NITRATE TRANSPORTER 1.1 (NRT1.1) and the
58 transcription-activating nitrate sensor NIN-LIKE PROTEIN 7 (NLP7) play central roles in PNR
59 (Ho et al. 2009; Bouguyon et al. 2015; Liu et al. 2017; Liu et al. 2022). Nitrate uptake via NRT1.1
60 transiently induces a Ca^{2+} influx, thereby elevating both cytosolic and nuclear Ca^{2+} levels (Riveras
61 et al. 2015; Liu et al. 2017; Wang et al. 2021). NRT1.1 physically interacts with the cyclic
62 nucleotide-gated channel CNGC15 to form a nitrate-activated Ca^{2+}-permeable channel on the
63 plasma membrane (Wang et al. 2021). Additionally, PHOSPHOLIPASE C also contributes to the
64 NRT1.1-mediated increase in cytoplasmic Ca^{2+} levels (Riveras et al. 2015). The nitrate-binding
65 affinity and uptake activity of NRT1.1 are tuned by specific protein kinases and phosphatase,
66 including CBL-INTERACTING PROTEIN KINASEs 8/23, SUCROSE NON-FERMENTING1-
67 RELATED PROTEIN KINASE (SnRK) 2s, and ABA INSENSITIVE 2 (Ho et al. 2009; Hu et al.
68 2009; Léran et al. 2015; Su et al. 2020). The subgroup III calcium-dependent protein kinases
69 10/30/32 (CPK10/30/32) perceive Ca^{2+} and phosphorylate NLP7 at S205, causing its nuclear
70 retention by inhibiting nuclear export (Marchive et al. 2013; Liu et al. 2017). Nitrate-bound NLP7,
71 along with transcription factors NLP2/6 and NITRATE REGULATORY GENE 2—which
72 physically interact with NLP7—promotes the transcription of PNR genes including those
73 encoding secondary transcription factors, thereby further altering the expression of downstream
74 target genes (Konishi and Yanagisawa 2013; Xu et al. 2016; Maeda et al. 2018; Liu et al. 2022;
75 Durand et al. 2023). Carbon deficiency leads to NLP7 depletion via SnRK1-mediated
76 phosphorylation, which promotes its degradation, thereby attenuating nitrate signaling (Wang et
77 al. 2022). This suggests that carbon availability modulates PNR.

78 Besides its role in PNR, nitrate acts as an internal signal of plant nitrogen status,
79 modulating nitrogen responses under steady-state conditions. In tobacco plants with different NR
80 activities grown under varying nitrate availability, the shoot-to-root dry weight ratio was
81 positively correlated with foliar nitrate levels (Scheible et al. 1997). In *Arabidopsis*, abundant
82 nitrate availability inhibits primary and lateral root growth (Zhang et al. 1998; Signora et al. 2001;
83 Patterson et al. 2016). Patterson et al. (2016) reported that nitrate application increases the shoot
84 expression of glutaredoxin (Grx) genes *GrxS3/4/5/8* via Arabidopsis response regulators (ARRs)
85 1/10/12 for cytokinin (CK) signaling, thereby inhibiting primary root growth. Kobayashi et al.
86 (2024) suggested that GrxS1–8 are candidate phloem-mobile signals from shoots to roots, and
87 they bind to TGACG-binding factor 1 (TGA1) and TGA4 (Alvarez et al. 2014) in roots, forming
88 a corepressor complex with TOPLESS to limit high-affinity nitrate uptake. Meanwhile, Ota et al.
89 (2020) discovered that under reduced shoot nitrogen, including nitrate depletion, C-terminally
90 encoded peptide downstream-like 2 (CEPDL2)—a Grx family protein also known as GrxS9—is
91 induced in the leaf vasculature and subsequently translocated to the roots. The co-activator
92 complex composed of CEPDL2, its homologs CEPD1/2, and TGA1/4 promotes root nitrate
93 uptake (Kobayashi et al. 2024). These findings imply that shoot nitrate status influences root
94 nitrogen acquisition.

95 In our previous study, to focus on the action of shoot nitrate status, we manipulated
96 shoot nitrate levels using wild-type *Arabidopsis* and an NR-null mutant (Okamoto et al. 2019).
97 Subsequent RNA-sequencing (RNA-seq) suggested that shoot nitrate accumulation alone
98 represses the expression of nitrogen starvation-inducible genes in shoots and roots. Notably, we
99 observed that shoot nitrate accumulation was accompanied by increases in the shoot expression
100 of adenylate *ISOPENTENYLTRANSFERASE 3* (*IPT3*) and the shoot levels of N^6-(Δ^2-isopentenyl)
101 adenine (iP)-type CKs, including iP ribotides (iPRPs), iP-7-*N*-glucoside (iP7G), and iP-9-*N*-
102 glucoside (iP9G) (Hachiya et al. 2020). Adenylate IPTs are key enzymes that catalyze the
103 formation of iPRPs using DMAPP as the isoprenoid donor and adenylates as acceptors

104 (Sakakibara 2021). iP riboside 5′-monophosphate (iPRMP) is then activated to bioactive free base
105 iP via either the one-step LONELY GUY (LOG) pathway or a two-step pathway involving 5'-
106 ribonucleotide phosphohydrolase GY3 and CK/purine riboside nucleosidase CPN1/NSH3
107 (Kojima et al. 2023; Wu et al. 2023). Nitrate-induced expression of *IPT3* is localized mainly in
108 phloem cells (Miyawaki et al. 2004; Takei et al. 2004a), and iP-type CKs, which are de novo
109 synthesized by IPT3, are phloem-mobile (Hirose et al. 2008; Bishopp et al. 2011). CKs are a class
110 of phytohormones that play central roles in regulating growth and development, such as
111 promoting cell division in shoots and repressing lateral root initiation (Werner et al. 2003; Laplaze
112 et al. 2007). Multiple transcriptome analyses have demonstrated that CKs regulate specific gene
113 sets across several tissues and organs (Bhargava et al. 2013). Hence, the systemic regulation of
114 growth and transcriptomic responses to shoot nitrate status may be mediated via IPT3-synthesized
115 iP-type CKs. Supporting this idea, several lines of evidence indicate both overlap and crosstalk
116 between nitrate and CK signaling. For instance, nitrate- and CK-responsive genes have been
117 found to partially overlap (Sakakibara et al. 2006). In addition, the nitrogen depletion-dependent
118 induction of shoot *CEPDL2* is enhanced by CKs translocated from roots (Ota et al. 2020).
119 Furthermore, *trans*-zeatin (*t*Z)-type CKs mediate preferential root growth in nitrate-rich patches
120 over nitrate-poor patches (Ruffel et al. 2011; Poitout et al. 2018). Based on this context, the
121 present study examined the systemic responses to shoot nitrate status and their dependence on
122 shoot IPT3. We developed a novel experimental system to manipulate nitrate levels and *IPT3*
123 expression in a shoot-specific manner using grafted plants derived from plants lacking NR and/or
124 IPT3. Using the shoots and roots of the grafted plants, growth analysis, CK species determination,
125 and RNA-seq were performed. Our results indicated that shoot nitrate accumulation enhances
126 shoot growth and alters the transcriptomes of shoots and roots, which is elaborately tuned by
127 shoot IPT3 in the opposite direction in shoots and roots. We herein present a scheme incorporating
128 shoot nitrate accumulation responses with shoot IPT3 and iP-type CKs.
129

130 **Materials and Methods**

131 **Plant materials**

132 In this study, we used *A. thaliana* accession Columbia (Col) as the control line; NR-null mutant
133 (NR-null, Wang et al. 2007), *IPT3*-knockout mutant (*ipt3*, Miyawaki et al. 2006), and
134 *IPT3/IPT5/IPT7*-knockout mutant (*ipt3,5,7*, Miyawaki et al. 2006); and a transgenic plant
135 expressing *GFP* driven by the *IPT3* promoter (*proIPT3:GFP*, Takei et al. 2004a). Homozygous
136 multiple mutants of NR-null *ipt3* and NR-null *proIPT3:GFP* were produced via crossing.

137

138 **Culture media**

139 Three different solid media were used for *in vitro* plant culture as follows: (i) 2.5 mM NH_4^+
140 medium, half-strength Murashige and Skoog (1/2MS) modified basal salt mixture without
141 nitrogen (M531; PhytoTech Labs, Lenexa, KS, USA) supplemented with 1.25 mM $(NH_4)_2SO_4$,
142 10.0 g L^{-1} sucrose, 1.0 g L^{-1} MES, and 4.0 g L^{-1} gellan gum (Fujifilm Wako, Osaka, Japan) and
143 adjusted to pH 6.7 with KOH; (ii) 10 mM NO_3^- and 2.5 mM NH_4^+ medium, 1/2MS modified
144 basal salt mixture without nitrogen (M531; PhytoTech Labs) supplemented with 10 mM KNO_3,
145 1.25 mM $(NH_4)_2SO_4$, 10.0 g L^{-1} sucrose, 1.0 g L^{-1} MES, and 4.0 g L^{-1} gellan gum (Fujifilm
146 Wako) and adjusted to pH 6.7 with KOH; and (iii) no nitrogen medium, 1/2MS modified basal
147 salt mixture without nitrogen (M531; PhytoTech Labs) supplemented with 2.0 g L^{-1} sucrose, 0.5
148 g L^{-1} MES, and 5.0 g L^{-1} gellan gum (Fujifilm Wako) and adjusted to pH 5.7 with KOH. It should
149 be noted that pH 6.7 was employed to mitigate ammonium toxicity under 2.5 mM NH_4^+ medium
150 (Hachiya et al. 2021b) and to promote better growth of NR-deficient plants under 10 mM NO_3^-
151 and 2.5 mM NH_4^+ medium (Wang et al. 2004).

152

153 **Transfer experiments using grafted plants**

154 To manipulate nitrate levels and *IPT3* expression in a shoot-specific manner, micrografting and
155 transfer experiments were performed using Col, NR-null, *ipt3*, NR-null *ipt3*, and *ipt3,5,7* plants

156 (Figure 1A, B). Surface-sterilized seeds were placed in the dark at 4°C for 3 days to break seed
157 dormancy. To ensure uniform growth regardless of the NR activity, approximately 120 seeds per
158 dish were sown in rectangle dishes (140 × 100 × 20 mm^3; Eiken Chemical Co. Ltd., Tokyo, Japan)
159 containing 50 mL of 2.5 mM NH_4^+ medium and grown vertically at 22°C for 4 days under a
160 photosynthetic photon flux density (PPFD) of 25 μmol m^{-2} s^{-1} with a 16/8-h light/dark cycle
161 (condition 1). Four-day-old seedlings were micrografted aseptically in rectangle dishes containing
162 50 mL of 2.5 mM NH_4^+ medium using four combinations of scions and rootstocks corresponding
163 to Col/*ipt3,5,7*, NR-null/*ipt3,5,7*, *ipt3*/*ipt3,5,7*, and NR-null *ipt3*/*ipt3,5,7* (scion line
164 name/rootstock line name) (Figure 1B). Notably, *ipt3,5,7* was used as the rootstock to avoid the
165 complementation of shoot-specific CK depletion in *ipt3* by root-derived CKs. The seedlings were
166 cut perpendicularly at the upper hypocotyl with an injection needle tip (NN-2613S; TERUMO,
167 Tokyo, Japan) on a membrane filter (HAWP04700; Merck Millipore, Darmstadt, Germany). The
168 obtained scion was connected with the partner rootstock through a 0.4-mm silicon microtube (1-
169 8194-04; AS ONE, Osaka, Japan). The grafted plants were incubated in a growth chamber at
170 27°C for 5 days under a PPFD of 50 μmol m^{-2} s^{-1} with a constant light (condition 2) and further
171 cultivated at 22°C for 24 h under a PPFD of 25 μmol m^{-2} s^{-1} with a 16/8-h light/dark cycle
172 (condition 3). Successfully grafted plants without adventitious root formation were selected for
173 size uniformity. RT-PCR with primers specific for *NIA1*, *NIA2*, *IPT3*, *IPT5*, *IPT7*, and *ACTIN2*
174 confirmed the successful generation of the desired grafted plants (Figure S1A, B). The grafted
175 plants were transferred to round dishes (diameter, 90 mm; depth, 20 mm; AS ONE) containing 30
176 mL of 10 mM NO_3^- and 2.5 mM NH_4^+ medium and grown for 24 h under a PPFD of 25 μmol
177 m^{-2} s^{-1} with a constant light to promote nitrate accumulation in the grafted plants (condition 4).
178 Finally, the plants were transferred to round dishes containing 30 mL of no nitrogen medium and
179 grown for 5 days under a PPFD of 25 μmol m^{-2} s^{-1} with a constant light (condition 5) to allow
180 nitrate accumulation in the shoots of NR-null/*ipt3,5,7* and NR-null *ipt3*/*ipt3,5,7* but not in
181 Col/*ipt3,5,7* and *ipt3*/*ipt3,5,7*. A low light intensity of 25 μmol m^{-2} s^{-1} was employed to mitigate

182 stress, given that high light intensity exacerbates stress caused by nitrogen depletion (Iwagami et
183 al. 2022). The surfaces of no nitrogen medium were covered with cellophane sheets to allow
184 nondestructive sampling of the roots (Hachiya et al. 2021a). It should be noted that all plants were
185 grown under identical external nitrogen conditions to ensure uniform biosynthesis of systemic
186 signaling molecules responsive to external nitrogen availability—such as tZ-type CKs (Osugi et
187 al. 2017) and CEP peptides (Tabata et al. 2014)—thereby isolating the systemic effects of shoot
188 nitrate status and enabling clearer interpretation of the results. Additionally, external nitrogen
189 sources such as ammonium could enrich internal organic nitrogen pools and inadvertently activate
190 various nitrogen signaling, potentially masking the effects of shoot nitrate accumulation. To avoid
191 this, we manipulated shoot nitrate levels without supplying external nitrogen to the plants
192 (condition 5).
193
194 **Growth analysis**
195 Shoots and roots were weighed on a precision balance (HR-202i; A&D, Tokyo, Japan), and shoots
196 were scanned at a resolution of 600 dpi (GT-X980; EPSON, Tokyo, Japan) to measure the rosette
197 diameter. Leaf blades were harvested from the shoots and scanned at a resolution of 600 dpi to
198 measure the blade area of the cotyledon and true leaf. The rosette diameter and leaf blade area
199 were measured using ImageJ version 1.52p (US National Institutes of Health, Bethesda, MD,
200 USA).
201
202 **Determination of the total nitrogen content**
203 The total nitrogen concentration was quantified as previously described (Monden et al. 2022).
204 Harvested shoots and roots were oven-dried at 80°C for 2 days, and the dried samples were
205 ground using a spoon and stored in a desiccator before use. The dried powder was weighed and
206 encapsulated in a tin boat. Nitrogen concentrations were measured using a CN analyzer (Vario
207 EL III; Elementar Analysensysteme GmbH, Hanau, Germany).

208

209 **Determination of the nitrate content**

210 Nitrate content was quantified as previously described (Okamoto et al. 2019) with slight
211 modifications. Frozen samples were ground with a Multi-Beads Shocker (Yasui Kikai, Osaka,
212 Japan) using zirconia beads (diameter, 5 mm). The powder samples were boiled with 10 volumes
213 of Milli-Q water at 100°C for 20 min. Five microliters of the supernatant or 5 μL of standard
214 solution as dilution series of potassium nitrate was mixed with 40 μL of 0.05% (w/v) salicylic
215 acid in sulfuric acid. The resulting mixture was then incubated at room temperature for 20 min.
216 A mock treatment of 40 μL of sulfuric acid alone was added to 5 μL of the supernatant. One
217 microliter of 8% (w/v) NaOH solution was added to the mixture, and the nitrate content was
218 determined by measuring the absorbance at 410 nm using a plate reader (CORONA SH-9000Lab,
219 Hitachi High-Tech Corp., Tokyo, Japan).

220

221 **Observation of fluorescent signals**

222 Fluorescent imaging was performed using an All-in-one fluorescence microscope (BZ-X710,
223 KEYENCE, Osaka, Japan) with a 4× objective (CFI Plan Fluor DL 4×/0.13, Nikon, Tokyo, Japan)
224 and a metal halide lamp (No. 91056, KEYENCE). A narrow-band GFP filter (ex. 480/20; em.
225 510/20, 49020, Chroma, Brattleboro, VT, USA) and Cy5 filter (ex. 620/60; em. 700/75, 49006,
226 Chroma) were used to detect the fluorescence of GFP and chlorophyll, respectively.

227

228 **Determination of CK species**

229 The extraction and determination of CKs were performed with slight modifications to the method
230 described by Kojima et al. (2009). Frozen tissue was ground into powder using a TissueLyser
231 (Qiagen, Hilden, Germany) with a 5 mm zirconia bead. Samples were extracted in 1 ml of
232 methanol : formic acid : water (15 : 1 : 4), with stable isotope-labeled internal standards. After
233 incubation at –30°C for ≥16 h, samples were centrifuged at 10,000 × *g*, for 15 min. The

234 supernatant was collected, and the pellet was re-extracted with 0.2 ml of the same solvent.
235 Combined extracts were purified using Oasis HLB 96-well plates (Waters, Milford, MA, USA)
236 on a STAR (HAMILTON, Reno, NV, USA), followed by evaporation and reconstitution in 1 ml
237 of 1 M formic acid. Fractionation was performed on an Oasis MCX 96-well plate (Waters). ABA,
238 auxins, and gibberellins were eluted with methanol (Elution 1); CK nucleotides with 0.35 M
239 ammonia (Elution 2); and CK nucleobases, nucleosides, and glucosides with 0.35 M ammonia in
240 60% methanol (Elution 3). All fractions were dried by evaporation. For CK analysis, Elution 3
241 was reconstituted in 50 µl of 0.1% acetic acid. Elution 2 was reconstituted in 0.84 ml of 0.1 M
242 CHES-NaOH (pH 9.8), treated with 1 U μl^{-1} of alkaline phosphatase (Oriental Yeast, Tokyo,
243 Japan), incubated at 37°C for 1 h, neutralized, desalted via Oasis HLB plate, evaporated, and
244 reconstituted in 50 µl of 0.1% acetic acid. CKs were analyzed using an ultra-performance liquid
245 chromatography–tandem quadrupole mass spectrometry system (AQUITY UPLC
246 System/XEVO-TQS; Waters) with an octadecylsilyl column (ACQUITY UPLC HSS T3, 1.8 µm,
247 2.1 mm × 100 mm; Waters). CK species were separated at a flow rate of 0.25 mL min-1 with
248 linear gradients of solvent A (0.06% acetic acid) and solvent B (0.06% acetic acid in methanol)
249 set according to the following profile: 0 min, 95% A + 5% B; 7min, 60%A + 40% B; 10 min, 1%
250 A + 99% B; 10 min, 1% A + 99% B; 13 min,95% A + 5% B.
251
252 **Determination of the total protein content**
253 The total protein content was determined as previously described (Hachiya et al. 2016). Frozen
254 samples were ground with a Multi-Beads Shocker using zirconia beads (diameter, 5 mm). Total
255 proteins were extracted with 10 vol. of Laemmli buffer (2% (w/v) SDS, 62.5 mM Tris-HCl
256 (pH 6.8), 10% (v/v) glycerol, and 0.0125% (w/v) bromophenol blue) containing Halt™ protease
257 inhibitor cocktail (Thermo Fisher Scientific, Waltman, MA, USA), followed by incubation at
258 95°C for 5 min. Extracts were centrifuged at 20,400 × *g* at room temperature for 10 min, and 10
259 µL of each aliquot was suspended in 500 µL of deionized water. Next, 100 µL of 0.15% (w/v)

260 sodium deoxycholate was added, and the mixture was incubated at room temperature for 10 min.
261 One hundred microliters of 72% (v/v) trichloroacetic acid was added, followed by incubation at
262 room temperature for 15 min and centrifugation at 20,400 × *g* for 10 min. The precipitates were
263 air-dried and suspended in 25 μL of deionized water. The suspension was analyzed with a TaKaRa
264 BCA Protein Assay Kit (T9300A, TaKaRa, Kusatsu, Japan) according to the manufacturer's
265 instructions. Protein content was determined by measuring the absorbance at 562 nm using a plate
266 reader (Hitachi High-Tech Corp.).
267
268 **RNA extraction**
269 Frozen samples were ground with a Multi-Beads Shocker using zirconia beads (diameter, 5 mm).
270 Total RNA was extracted using an RNeasy Plant Mini Kit (Qiagen) according to the
271 manufacturer's instructions. For RNA-seq library preparation, RNA was purified via on-column
272 DNase digestion (Qiagen).
273
274 **RNA-seq**
275 RNA quality was evaluated using a Qubit RNA IQ Assay Kit with a Qubit 4 Fluorometer (Thermo
276 Fisher Scientific). The RNA samples for which the RNA IQs ranged 9.4–10.0 were used for RNA-
277 seq. cDNA libraries were constructed using a NEBNext Ultra II RNA Library Prep with Sample
278 Purification Beads (E7775S, New England Biolabs, Ipswich, MA, USA), a NEBNext Poly(A)
279 mRNA Magnetic Isolation Module (E7490S, New England Biolabs), and a NEBNext Multiplex
280 Oligos for Illumina (E7710S, New England Biolabs) according to the manufacturer's instructions.
281 These cDNA libraries were sequenced using NextSeq 500 (Illumina, San Diego, CA, USA), and
282 the produced bcl files were converted to fastq files using bcl2fastq (Illumina). The reads were
283 analyzed according to a previously described method (Notaguchi et al. 2014) and mapped to the
284 Arabidopsis reference (TAIR10) using Bowtie (Langmead et al. 2009) with the following options:
285 "--all --best --strata." The mapped reads were processed using iDEP version 0.96 and 2.01 (Ge et

286 al. 2018). For data normalization, the read counts data were transformed with rlog and normalized
287 by subtracting the average expression for each gene according to the default setting of iDEP. For
288 DEG extraction, DESeq2 was run with a false-discovery rate cutoff of 0.1. The enrichment
289 analysis of each gene set was conducted using Metascape (Zhou et al. 2019) according to the
290 default setting.
291
292 **RT-qPCR**
293 Reverse transcription (RT) was performed using a ReverTraAce qPCR RT Master Mix with
294 gDNA Remover (Toyobo, Osaka Japan). RNA solution containing 0.5 µg of template RNA
295 served as the input. Synthesized cDNA was then diluted 5-fold with water and used for
296 quantitative PCR (qPCR). RT-qPCR was performed on a QuantStudio 1 (Thermo Fisher
297 Scientific) with KOD SYBR qPCR Mix (Toyobo). Relative transcript levels were calculated
298 using the comparative cycle threshold method, with *ACTIN3* as the internal standard (Hachiya et
299 al. 2021b). Primer sequences are presented in Table S1.
300
301 **Statistical analysis**
302 Unpaired two-tailed Welch's *t*-test and Tukey–Kramer multiple comparison test were performed
303 using R software v.2.15.3 (R Foundation for Statistical Computing, Vienna, Austria).
304
305 **Results and discussion**
306 **Manipulation of nitrate levels and *IPT3* expression in a shoot-specific manner**
307 After nitrogen removal (condition 5), nitrate concentrations generally decreased over time in the
308 shoots and roots of all plants (Figure 1C, D). At 3 and 5 days after nitrogen removal, the shoot
309 nitrate concentrations were higher in NR-null/*ipt3,5,7* and NR-null *ipt3*/*ipt3,5,7* plants than in the
310 other plants (Figure 1C), whereas root nitrate was depleted to the same level in all plants (Figure
311 1D). Meanwhile, at 5 days after nitrogen removal, total protein and total nitrogen levels in shoots

312 and roots differed little among the plants (Figure 1E–H). RT-qPCR revealed that shoot *IPT3*
313 expression was significantly higher in NR-null/*ipt3,5,7* than in Col/*ipt3,5,7* (Figure 1I). Only
314 minor differences in transcripts per million (TPM) of shoot *IPT1/4/5/6/7/8* and root *IPT1/4/6/8*
315 were observed among the four grafted plants (Figure S1C), suggesting that adenylate *IPT* genes
316 other than *IPT3* did not compensate for the absence of shoot IPT3. To visualize the tissue-specific
317 induction of *IPT3* as a result of shoot NR deficiency, scions from *proIPT3:GFP* and NR-null
318 *proIPT3:GFP* plants were grafted onto *ipt3,5,7* rootstocks, followed by the same transfer
319 experiment as before. Shoot nitrate accumulation and *GFP* induction were observed in NR-null
320 *proIPT3:GFP*/*ipt3,5,7* plants 5 days after nitrogen removal (Figure 1J, K), with strong GFP
321 fluorescence localized in the leaf vein (Figure 1L). These findings suggest that *IPT3* induction
322 due to shoot nitrate accumulation occurs mainly in the vasculature. Given that NLP7 promotes
323 the *IPT3* transcription in response to exogenous nitrate application (Maeda et al. 2018; Liu et al.
324 2022), it is plausible that *IPT3* induction in NR-null/*ipt3,5,7* is also mediated by NLP7. Overall,
325 we successfully developed a novel system that manipulates nitrate levels and *IPT3* expression in
326 a shoot-specific manner, with minimal impact on the total protein and total nitrogen levels within
327 the plant, in the absence of external nitrogen sources. This system allows the analysis of systemic
328 responses to shoot nitrate status and their dependence on shoot IPT3 in the following experiments.
329 All experiments described below were conducted using samples collected 5 days after nitrogen
330 removal (condition 5).
331
332 **Shoot nitrate accumulation elevates shoot levels of iP-type CKs via shoot IPT3**
333 To assess the impact of shoot nitrate status and shoot *IPT3* expression on CK activity, we
334 measured the concentrations of iP-type and *t*Z-type CKs. The experiments were performed using
335 the shoots and roots of grafted plants, with three biological replicates collected independently
336 (Figure 2) or simultaneously (Figure S2). The levels of iPRPs, iP7G, iP9G, *t*Z ribotides (*t*ZRPs),
337 *t*Z-7-*N*-glucoside (*t*Z7G), *t*Z-9-*N*-glucoside (*t*Z9G), *t*Z-*O*-glucoside (*t*ZOG), and *t*ZR-*O*-

338 glucoside (*t*ZROG) were consistently lower in the shoots of *ipt3*/*ipt3,5,7* and NR-null
339 *ipt3*/*ipt3,5,7* plants than in those of Col/*ipt3,5,7* and NR-null/*ipt3,5,7* plants (Figure 2C–E, 2H–L
340 and Figure S2C–E, S2H–L). Meanwhile, little difference was observed in the root levels of CK
341 species among the grafted plants. These observations indicated that shoot IPT3 is crucial for
342 maintaining the shoot levels of *t*Z-type and iP-type CKs, but it has only a minor effect on root CK
343 levels. Notably, the shoot levels of iPRPs, iP7G, and iP9G were significantly increased by shoot
344 NR deficiency in the presence of shoot IPT3 but not in its absence (Figure 2C–E and Figure S2C–
345 E). This finding suggests that shoot nitrate accumulation elevates the shoot levels of these iP-type
346 CKs via shoot IPT3. However, no significant increase was observed in the levels of iP, the
347 biologically active form (Figure 2A and Figure S2A). In *Arabidopsis*, seven LOG enzymes with
348 phosphoribohydrolase activity can directly convert iPRMP into iP (Kuroha et al. 2009; Tokunaga
349 et al., 2011). Thus, elevated levels of iPRPs in the shoot likely serve as a reservoir of latent CK
350 activity, with the potential to promote growth depending on the spatial and temporal activity of
351 LOG enzymes. Given that Arabidopsis *LOG* genes exhibit distinct spatial expression patterns
352 (Kuroha et al. 2009), the iPRPs accumulated in response to shoot nitrate accumulation may be
353 locally converted to iP in cells or tissues expressing specific LOG isoforms. While our CK
354 quantifications were performed using whole shoots and roots, it is possible that localized changes
355 in iP concentrations—especially in actively growing regions such as the shoot apical meristem or
356 the basal zone of young leaves—were not captured. Targeted sampling of these regions may
357 therefore be necessary to reveal the spatial dynamics of iP production in response to shoot nitrate
358 status.
359
360 **Shoot nitrate accumulation enhances shoot growth via shoot IPT3**
361 To determine the effects of shoot nitrate status and shoot *IPT3* expression on plant growth, we
362 analyzed growth parameters using all grafted plants from five independent experiments (Figure
363 3). Shoot fresh weight, leaf blade area, rosette diameter, and leaf number were significantly lower

364 in *ipt3*/*ipt3,5,7* and NR-null *ipt3*/*ipt3,5,7* plants than in Col/*ipt3,5,7* and NR-null/*ipt3,5,7* plants
365 (Figure 3B–E). Meanwhile, no significant difference was observed in the root fresh weight among
366 the grafted plants (Figure 3F). These observations indicate that shoot IPT3 generally contributes
367 to shoot growth. Importantly, shoot appearance, shoot fresh weight, and leaf blade area were
368 significantly increased by shoot NR deficiency in the presence of shoot IPT3 but not in its absence
369 (Figure 3A–C). A similar trend was observed for the rosette diameter, although the differences
370 were not statistically significant (Figure 3D). These patterns correspond to the findings for shoot
371 iPRPs, iP7G, and iP9G concentrations (Figure 2C–E and Figure S2C–E). Actually, shoot fresh
372 weight and leaf blade area were strongly correlated with levels of these iP-type CKs (Figure S3).
373 Overall, these findings suggest that shoot nitrate accumulation promotes shoot growth by
374 increasing IPT3 and iP-type CK biosynthesis in the shoot. It is well established that in Arabidopsis
375 plants, root-supplied nitrate stimulates the biosynthesis of *t*Z-type CKs in the root and facilitates
376 their transport to the shoot, thereby promoting shoot growth (Kiba et al. 2013; Osugi et al. 2017;
377 Sakakibara, 2021). Meanwhile, in the present study, shoot nitrate accumulation did not
378 significantly increase *t*Z-type CK levels in both shoots and roots (Figure 2F–M and Figure S2F–
379 M), arguing against their involvement in shoot growth regulation in response to internal nitrate
380 status. Interestingly, the fresh weight ratios of shoot to root were elevated by shoot NR deficiency
381 in the presence of shoot IPT3 but not in its absence (Figure 3G). Given that, in general, biomass
382 ratios of shoot to root are positively correlated with overall nitrogen availability within and
383 outside the plants (Andrews et al. 2006; Krapp et al. 2011; Hachiya et al. 2014), our findings
384 support the idea that shoot nitrate status serves as an indicator of nitrogen availability.
385 Furthermore, since CK action is known to enhance sink activity in shoots (Werner et al. 2008), it
386 is plausible that shoot nitrate status influences biomass allocation between shoot and root via
387 shoot IPT3-mediated CK signaling.
388

Transcriptomic responses to shoot nitrate accumulation are tuned via shoot IPT3 with opposite effects in shoots and roots

To investigate the effects of shoot nitrate status and shoot *IPT3* expression on systemic responses, we performed RNA-seq using the shoots and roots of grafted plants, with three biological replicates collected independently. Reads per million mapped reads (RPM; Table S2) and normalized transcript levels (Table S3) were calculated according to the read counts. To identify genes regulated by shoot nitrate accumulation and further modulated by shoot IPT3, we extracted differentially expressed genes (DEGs) between NR-null/*ipt3,5,7* and Col/*ipt3,5,7* and between NR-null *ipt3*/*ipt3,5,7* and *ipt3*/*ipt3,5,7* with a minimum fold change of 1.5 (Figure 4A and Figure S4 and Table S4). Comparison of these DEGs between shoots and roots revealed minimal overlap (Figure S4), indicating that shoots and roots express distinct sets of genes regulated by shoot nitrate accumulation. Hence, we analyzed the shoot and root transcriptomes separately. Notably, ~~I~~in shoots, the number of DEGs was larger between NR-null/*ipt3,5,7* and Col/*ipt3,5,7* than between NR-null *ipt3*/*ipt3,5,7* and *ipt3*/*ipt3,5,7* (Figure 4A). By contrast, in roots, the number of DEGs was lower between NR-null/*ipt3,5,7* and Col/*ipt3,5,7* than between NR-null *ipt3*/*ipt3,5,7* and *ipt3*/*ipt3,5,7* (Figure 4A). The shoot transcriptional responses of 631 and 663 DEGs to shoot NR deficiency were decreased by shoot IPT3 deficiency (Figure 4B, C), whereas the root responses of 189 and 126 DEGs were augmented by shoot IPT3 deficiency (Figure 4D, E). Three independent RNA-seq results exhibited similar trends; therefore, only the mean transcript levels are presented in subsequent figures for clarity, unless otherwise stated. k-means clustering identified 11 out of 16 clusters (clusters 1, 2, 3, 6, 7, 8, 11, 12, 14, 15, and 16) in which gene expression was significantly altered by shoot NR deficiency, with their responses decreased by shoot IPT3 deficiency in shoots but increased in roots (Figure S5, S6 and Table S5). In summary, shoot transcriptional responses to shoot nitrate accumulation are generally enhanced by shoot IPT3, whereas root responses are dampened by shoot IPT3.

414 Enrichment analyses of the 11 clusters from Figure S5 and S6 revealed a diverse set
415 of genes significantly regulated by shoot nitrate and shoot IPT3. In shoots, the cluster 6 and 8
416 enriched terms related to translation, primary carbon metabolism, and biotic stress response such
417 as "ath03010: Ribosome", "WP2621: Glycolysis", and "GO:0009617: response to bacterium"
418 (Figure S5A). Previously, we reported that shoot nitrate accumulation is accompanied by the
419 upregulation of ribosome-associated genes in shoots (Hachiya et al. 2020). It is widely known
420 that CK signal upregulates genes encoding ribosomal proteins and elongation factors (Sakakibara
421 et al. 2006). Hence, translation may be activated by shoot nitrate accumulation, some of which
422 are mediated by shoot IPT3 (Figure S5B). Meanwhile, terms related to wounding and jasmonic
423 acids were overrepresented in both cluster 3 and 7 (Figure S5A). Thus, stress responses associated
424 with jasmonic acids signaling could be downregulated by shoot nitrate accumulation, which is
425 enhanced by shoot IPT3 (Figure S5B). In roots, the cluster 11, 12, and 14 predominantly featured
426 terms related to abiotic and biotic stresses, particularly hypoxia (Figure S6A). The cluster 15 and
427 16 enriched terms associated with translation, biosynthesis, and nitrate transport (Figure S6A).
428 Notably, the genes encoding nitrate reductases (*NIA1*, *NIA2*) and high-affinity nitrate transporters
429 (*NRT2.1*, *NRT2.4*, *NRT2.5*, *NRT3.1*) were included in the cluster 16 (Table S5). Thus, shoot
430 nitrate accumulation suppresses anabolism including nitrogen assimilation in the roots, the
431 responses of which are dampened by shoot IPT3 (Figure S6B).
432
433 **Shoot nitrate accumulation induces shoot *ARR2* expression via shoot IPT3**
434 We examined the shoot expression of CK-inducible genes using a shared list across multiple
435 studies (Bhargava et al. 2013). However, our survey failed to detect their transcriptional changes
436 associated with shoot NR and/or IPT3 deficiency (Figure S7A and Table S6). Notably, previous
437 studies analyzed early transcriptomic responses to exogenous application of *t*Z and benzyladenine
438 (Bhargava et al. 2013); therefore, conventional gene lists might be unsuitable for evaluating
439 steady-state responses to alterations of endogenous iP-type CKs. Our meticulous investigation

440 discovered that shoot expression of the type-B response regulator gene *ARR2* was induced by
441 shoot NR deficiency in the presence of shoot IPT3 but not in its absence (Figure S7B), a finding
442 corroborated by RT-qPCR (Figure S7C). Choi et al. (2010) demonstrated that CK-activated
443 ARR2 enhances Arabidopsis immunity through direct binding with the transcription factor TGA3.
444 In Figure S5A, the cluster 8 derived from clustering was overrepresented in terms such as
445 "GO:0009617: response to bacterium" and "GO:0009627: systemic acquired resistance" (Figure
446 S5A). Thus, shoot nitrate accumulation might enhance immunity by upregulating *ARR2* via shoot
447 IPT3. Furthermore, given that *ARR2*-overexpressing plants exhibit larger rosette leaves and
448 biomass (Arnaud et al. 2017), it is plausible that shoot nitrate accumulation could promote shoot
449 growth partly via shoot IPT3–ARR2 cascade.
450

451 **Transcriptional responses of nitrate–CPKs–NLPs-regulatory genes to shoot nitrate**
452 **accumulation are enhanced via shoot IPT3**

453 Previously, we reported that the expression of nitrate-responsive genes is influenced by shoot
454 nitrate accumulation (Okamoto et al. 2019), prompting our focus on these genes. In shoots, the
455 transcript levels of genes induced by nitrate itself (Wang et al. 2004) were significantly increased
456 by shoot NR deficiency, and this induction was attenuated by shoot IPT3 deficiency (Figure 5A
457 and Table S7). By contrast, there was minimal variation in the root expression of nitrate-inducible
458 genes among the plants. Given that CPK10/30/32, NLP7, and its homologs (NLPs) govern nitrate-
459 dependent gene expression (Liu et al. 2017; Liu et al. 2022), we analyzed the expression of genes
460 induced by nitrate–CPKs–NLPs signaling. In shoots, the genes induced via CPK10/30/32 and
461 those co-induced via all NLPs exhibited similar expression patterns as the nitrate-inducible genes
462 (Figure 5A–C and Table S7). Meanwhile, none of the genes induced exclusively by individual
463 NLPs exhibited different expression patterns among the plants (Figure S8 and Table S8). In roots,
464 the expression of genes regulated via CPK10/30/32 and NLPs showed little variation among the
465 plants (Figure 5B, C and Figure S8 and Table S7, S8). These findings suggest that shoot nitrate

466 accumulation upregulates nitrate-inducible genes via CPK10/30/32 and multiple NLPs
467 specifically in the shoots, with their responses enhanced by shoot IPT3.
468
469 **Transcriptional responses of nitrogen starvation-inducible genes to shoot nitrate**
470 **accumulation are tuned via shoot IPT3 in the opposite direction in shoots and roots**
471 Previously, we reported that shoot nitrate accumulation alleviates nitrogen starvation responses
472 (Okamoto et al. 2019). Thus, we analyzed the responses of two independent sets of nitrogen
473 starvation-inducible gene (Krapp et al. 2011; Kiba et al. 2018) (Table S9). Although these gene
474 sets are quite distinct (Figure S9A), shoot NR deficiency consistently repressed shoot expression
475 of nitrogen starvation-inducible genes, with this repression slightly alleviated by shoot IPT3
476 deficiency (Figure S9B, C). The nitrogen starvation-inducible genes common to both gene sets
477 exhibited a similar but stronger tendency (Figure 5D). Meanwhile, the root expression of nitrogen
478 starvation inducible-genes were significantly repressed by shoot NR deficiency only in the
479 absence of shoot IPT3 (Figure 5D and S9B, C). Overall, the repression of nitrogen starvation-
480 inducible genes to shoot nitrate accumulation is enhanced by shoot IPT3 in the shoot, but
481 dampened in the root.
482 Several genes involved in nitrogen transport and assimilation in the root are often
483 induced under nitrogen starvation (Krapp et al. 2011; Kiba et al. 2018), and thus, we focused on
484 their root expression. Most of the genes involved in high-affinity nitrate transport and nitrogen
485 assimilation were slightly downregulated by shoot NR deficiency, and these responses were
486 remarkably intensified by shoot IPT3 deficiency (Figure 5E). Thus, the degree of downregulation
487 in root nitrate utilization due to shoot nitrate accumulation is largely dependent on shoot IPT3.
488 By contrast, genes involved in dual-affinity/low-affinity nitrate transport (*NRT1.1* and *NRT1.2*)
489 (Liu et al. 1999) were upregulated by shoot NR deficiency regardless of the presence of shoot
490 IPT3 (Figure 5E). Because NRT1.1 and NRT1.2 can facilitate the uptake of auxin and abscisic

491 acid, respectively (Krouk et al. 2010; Kanno et al. 2012), their upregulation may not necessarily
492 be related to nitrate acquisition.
493
494 **Systemic regulation of nitrogen starvation-inducible genes regulated by shoot nitrate**
495 **accumulation may be mediated via transcriptional repressors and mobile peptides**
496 Nitrate signaling induces nitrate-inducible GARP-type transcriptional repressor 1 clade genes
497 (*NIGT1.1/1.2/1.3/1.4*) and *LOB DOMAIN-CONTAINING PROTEIN 37/38/39* genes
498 (*LBD37/38/39*) via NLPs (Rubin et al. 2009; Marchive et al. 2013; Kiba et al. 2018; Maeda et al.
499 2018; Safi et al 2021). These translational products act as repressors to downregulate nitrogen
500 starvation-inducible genes. Thus, we examined these repressor genes. In the shoot, the transcript
501 levels of *NIGT1.1* and *LBD37/38* were increased by shoot NR deficiency, and this induction was
502 attenuated by shoot IPT3 deficiency (Figure 5F and S10A). The expression of these repressors
503 exhibited a strong negative correlation with that of nitrogen starvation-inducible genes in the
504 shoot (Figure S10B). In the root, the transcript levels of *NIGT1.1/1.2* and *LBD37/38* were
505 increased by shoot NR deficiency, and this induction was enhanced by shoot IPT3 deficiency
506 (Figure 5G and S10C). Interestingly, root *LBD39* expression was induced by shoot NR deficiency
507 only in the absence of shoot IPT3. These repressors also showed a strong negative correlation
508 with nitrogen starvation-inducible genes in the root (Figure S10D). These findings suggest that
509 shoot nitrate accumulation and shoot IPT3 regulate the systemic regulation of nitrogen starvation-
510 inducible genes via these repressors. It is valuable to explore whether iP-type CKs synthesized
511 by shoot IPT3 systemically regulate the root expression of repressor genes.
512 Next, we focused on candidate shoot-to-root mobile peptides regulating systemic
513 nitrogen responses, i.e., CEPD1/2, CEPDL2, and GrxS1–8 (Ohkubo et al. 2017; Ota et al. 2020;
514 Kobayashi et al. 2024) (Figure 5H and S11). The co-activator complexes composed of
515 CEPD1/2/CEPDL2 and TGA1/4 promote root nitrate uptake via upregulation of *NRT2.1* and
516 *CEPH*, whereas the co-repressor complexes of GrxS1–8 and TGA1/4 repress it (Kobayashi et al.

517 2024). In the shoot, *CEPDL2* transcript levels were markedly reduced by shoot NR deficiency,
518 and this repression was attenuated by shoot IPT3 deficiency (Figure 5H and S11A). In contrast,
519 shoot *GrxS3* expression was upregulated by shoot NR deficiency, and this induction was slightly
520 enhanced in the absence of shoot IPT3. Interestingly, shoot *GrxS5* expression was induced by
521 shoot NR deficiency only in the absence of shoot IPT3. The root expression of *NRT2.1* and *CEPH*
522 was positively correlated with shoot expression of *CEPDL2*, whereas negatively correlated with
523 shoot expression of *GrxS3* and *GrxS5* (Figure 5H and S11). These findings suggest that shoot
524 nitrate accumulation and shoot IPT3 regulate the systemic regulation of root high-affinity nitrate
525 uptake via the action of shoot-to-root mobile peptides.
526
527 **Conclusion: a scheme integrating shoot nitrate accumulation responses with shoot IPT3**
528 Our experimental system elucidated the systemic responses to shoot nitrate status and their
529 dependence on shoot IPT3. A novel scheme for the systemic responses is summarized in Figure
530 6: shoot nitrate accumulation enhances shoot growth and the shoot expression of *IPT3*, nitrate–
531 CPKs–NLPs-inducible genes including nitrate uptake/assimilation genes, and immune response
532 genes, with their responses enhanced by shoot IPT3. Meanwhile, shoot nitrate accumulation
533 decreases the root expression of nitrogen starvation-inducible genes and nitrate
534 uptake/assimilation genes, with their responses dampened by shoot IPT3. Hence, under shoot
535 nitrate accumulation, shoot IPT3 would promote nitrogen utilization at the whole-plant scale,
536 providing organic nitrogen crucial for shoot growth enhancement. Notably, plant CK levels are
537 generally reduced by prolonged abiotic stresses including salinity, drought, chilling, and heat
538 (Cortleven et al. 2019), during which shoot growth is usually suppressed. Thus, shoot growth and
539 nitrogen utilization, which are tuned by shoot IPT3 depending on shoot nitrate status, would be
540 further fine-tuned via modulation of CK levels depending on abiotic stresses. Such crosstalk in
541 CK signaling would optimize plant growth and nitrogen utilization in fluctuating environments.
542 Despite these insights, it remains challenging to distinguish between primary and secondary

responses to shoot nitrate accumulation, as well as to evaluate the potential effects of organic nitrogen compounds such as Gln, a candidate nitrogen status signal (Nacry et al., 2013), which were not quantified in this study. In addition, it is unclear exactly where and how the phloem-mobile iP-type CKs produced by shoot IPT3 trigger downstream signaling to orchestrate systemic responses. Furthermore, the cell types, subcellular compartments, and molecular mechanisms involved sensing shoot nitrate status are entirely unknown. Future work needs to meticulously investigate these unresolved questions.

Author contributions

TH: conceptualization; TS: data curation; KM and TH: formal analysis; KM and TH: funding acquisition; KM, TS, MK, YT, and DS: investigation; KM: methodology; KM and TH: project administration; KM and TH: resources; TN, HS, and TH: supervision; KM and TH: validation; KM and TH: visualization; TH: writing – original draft preparation; All authors: writing – review & editing.

Acknowledgements

The NR-null seeds were kindly provided by Dr. Nigel M. Crawford (University of California, San Diego). The *ipt3* and *ipt3,5,7* seeds were kindly provided by Dr. Tatsuo Kakimoto (Osaka University). We thank Ms. Yuki Okamoto and Mr. Masahiro Watanabe for their support in the preparation of the plant materials. This study was supported by JSPS KAKENHI [No. 20K05771 and 23K04978 to TH and No. JP24KJ1709 to KM], by JST SPRING [No. JPMJSP2155 to KM], and by the Sasakawa Scientific Research Grant from the Japan Science Society [No. 2022-4039 to KM].

Conflicts of interest

The authors declare no competing interests.

569

570 **Data Availability Statement**

571 The RNA-seq raw data are available in ArrayExpress under the accession number E-MTAB-
572 14302 (https://www.ebi.ac.uk/biostudies/arrayexpress).

573

574 **References**

575 Alvarez, J. M., E. Riveras, E. A. Vidal, et al. 2014. "Systems approach identifies TGA1 and TGA4
576 transcription factors as important regulatory components of the nitrate response of *Arabidopsis*
577 *thaliana* roots." *Plant Journal* 80 : 1–13. https://doi.org/10.1111/tpj.12618.

578

579 Andrews, M., J. A. Raven, P. J. Lea, and J. I. Sprent. 2006. "A role for shoot protein in shoot–
580 root dry matter allocation in higher plants." *Annals of Botany* 97: 3–10.
581 https://doi.org/10.1093/aob/mcj009.

582

583 Arnaud, D., S. Lee, Y. Takebayashi, et al. 2017. "Cytokinin-mediated regulation of reactive
584 oxygen species homeostasis modulates stomatal immunity in Arabidopsis." *Plant Cell* 29: 543–
585 559. https://doi.org/10.1105/tpc.16.00583.

586

587 Bhargava, A., I. Clabaugh, J. P. To, et al. 2013. "Identification of cytokinin-responsive genes
588 using microarray meta-analysis and RNA-Seq in Arabidopsis." *Plant Physiology* 162: 272–294.
589 https://doi.org/10.1104/pp.113.217026.

590

591 Bishopp, A., S. Lehesranta, A. Vatén, et al. 2011. "Phloem-transported cytokinin regulates polar
592 auxin transport and maintains vascular pattern in the root meristem." *Current Biology* 21: 927–
593 932. https://doi.org/10.1016/j.cub.2011.04.049.

594

595 Bouguyon, E., F. Brun, D. Meynard, et al. 2015. "Multiple mechanisms of nitrate sensing by
596 *Arabidopsis* nitrate transceptor NRT1.1." *Nature Plants* 1: 15015.
597 https://doi.org/10.1038/nplants.2015.15.
598
599 Choi, J., S. U. Huh, M. Kojima, H. Sakakibara, K. H. Paek, and I. Hwang. 2010. "The cytokinin-
600 activated transcription factor ARR2 promotes plant immunity via TGA3/NPR1-dependent
601 salicylic acid signaling in *Arabidopsis*." *Developmental Cell* 19: 284–295.
602 https://doi.org/10.1016/j.devcel.2010.07.011.
603
604 Cortleven, A., J. E. Leuendorf, M. Frank, D. Pezzetta, S. Bolt, and T. Schmülling. 2019.
605 "Cytokinin action in response to abiotic and biotic stresses in plants." *Plant, Cell & Environment*
606 42: 998–1018. https://doi.org/10.1111/pce.13494.
607
608 Durand, M., V. Brehaut, G. Clement, et al. 2023. "The Arabidopsis transcription factor NLP2
609 regulates early nitrate responses and integrates nitrate assimilation with energy and carbon
610 skeleton supply." *Plant Cell* 35: 1429–1454. https://doi.org/10.1093/plcell/koad025.
611
612 Ge, S. X., E. W. Son, and R. Yao. 2018. "iDEP: an integrated web application for differential
613 expression and pathway analysis of RNA-Seq data." *BMC Bioinformatics* 19: 534.
614 https://doi.org/10.1186/s12859-018-2486-6.
615
616 Hachiya, T., D. Sugiura, M. Kojima, et al. 2014. "High CO_2 triggers preferential root growth of
617 *Arabidopsis thaliana* via two distinct systems under low pH and low N stresses." *Plant & Cell*
618 *Physiology* 55: 269–280. https://doi.org/10.1093/pcp/pcu001.
619
620 Hachiya, T., N. Ueda, M. Kitagawa, et al. 2016. "Arabidopsis root-type ferredoxin:NADP(H)

621 oxidoreductase 2 is involved in detoxification of nitrite in roots." *Plant & Cell Physiology* 57:
622 2440–2450. https://doi.org/10.1093/pcp/pcw158.
623
624 Hachiya, T., and H. Sakakibara. 2017. "Interactions between nitrate and ammonium in their
625 uptake, allocation, assimilation, and signaling in plants." *Journal of Experimental Botany* 68:
626 2501-2512. https://doi.org/10.1093/jxb/erw449.
627
628 Hachiya, T., Y. Okamoto, M. Watanabe, et al. 2020. "Genome-wide responses to shoot nitrate
629 satiety are attenuated by external ammonium in *Arabidopsis thaliana*." *Soil Science and Plant*
630 *Nutrition* 66: 317–327. https://doi.org/10.1080/00380768.2020.1717905.
631
632 Hachiya, T., T. Oya, K. Monden, A. Nagae, and T. Nakagawa. 2021a. "A cellophane-supported
633 *Arabidopsis* culture for seamless transfer between different media is useful for studying various
634 nitrogen responses." *Soil Science and Plant Nutrition* 67: 277–282.
635 https://doi.org/10.1080/00380768.2021.1908094.
636
637 Hachiya, T., J. Inaba, M. Wakazaki, et al. 2021b. "Excessive ammonium assimilation by plastidic
638 glutamine synthetase causes ammonium toxicity in *Arabidopsis thaliana*." *Nature*
639 *Communications* 12: 4944. https://doi.org/10.1038/s41467-021-25238-7.
640
641 Hirose, N., K. Takei, T. Kuroha, T. Kamada-Nobusada, H. Hayashi, and H. Sakakibara. 2008.
642 "Regulation of cytokinin biosynthesis, compartmentalization and translocation." *Journal of*
643 *Experimental Botany* 59: 75–83. https://doi.org/10.1093/jxb/erm157.
644
645 Ho, C. H., S. H. Lin, H. C. Hu, and Y. F. Tsay. 2009. "CHL1 functions as a nitrate sensor in
646 plants." *Cell* 138: 1184–1194. https://doi.org/10.1016/j.cell.2009.07.004.

647

648 Hu, H. C., Y. Y. Wang, and Y. F. Tsay. 2009. "AtCIPK8, a CBL-interacting protein kinase,
649 regulates the low-affinity phase of the primary nitrate response." *Plant Journal* 57: 264–278.
650 https://doi.org/10.1111/j.1365-313X.2008.03685.x.

651

652 Kanno, Y., A. Hanada, Y. Chiba, et al. 2012. "Identification of an abscisic acid transporter by
653 functional screening using the receptor complex as a sensor." *Proceedings of the National*
654 *Academy of Sciences of the United States of America* 109: 9653–9658.
655 https://doi.org/10.1073/pnas.120356710.

656

657 Kiba, T., K. Takei, M. Kojima, and H. Sakakibara. 2013. "Side-chain modification of cytokinins
658 controls shoot growth in *Arabidopsis*." *Developmental Cell* 27: 452–461.
659 https://doi.org/10.1016/j.devcel.2013.10.004.

660

661 Kiba, T., J. Inaba, T. Kudo, et al. 2018. "Repression of nitrogen starvation responses by members
662 of the Arabidopsis GARP-type transcription factor NIGT1/HRS1 subfamily." *Plant Cell* 30: 925–
663 945. https://doi.org/10.1105/tpc.17.00810.

664

665 Ko, D., J. Kang, T. Kiba, et al. 2014. "*Arabidopsis* ABCG14 is essential for the root-to-shoot
666 translocation of cytokinin." *Proceedings of the National Academy of Sciences of the United States*
667 *of America* 111: 7150–7155. https://doi.org/10.1073/pnas.132151911.

668

669 Kobayashi, R., Y. Ohkubo, M. Izumi, et al. 2024. "Integration of shoot-derived polypeptide
670 signals by root TGA transcription factors is essential for survival under fluctuating nitrogen
671 environments." *Nature Communications* 15: 6903. https://doi.org/10.1038/s41467-024-51091-5.

672

673 Kojima, M., T. Kamada-Nobusada, H. Komatsu, et al. 2009. "Highly sensitive and high-
674 throughput analysis of plant hormones using MS-probe modification and liquid chromatography–
675 tandem mass spectrometry: an application for hormone profiling in *Oryza sativa*." *Plant & Cell*
676 *Physiology* 50: 1201–1214. https://doi.org/10.1093/pcp/pcp057.
677
678 Kojima, M., N. Makita, K. Miyata, et al. 2023. "A cell wall–localized cytokinin/purine riboside
679 nucleosidase is involved in apoplastic cytokinin metabolism in *Oryza sativa*." *Proceedings of the*
680 *National Academy of Sciences of the United States of America* 120: e2217708120.
681 https://doi.org/10.1073/pnas.221770812.
682
683 Konishi, M., and S. Yanagisawa. 2013. "Arabidopsis NIN-like transcription factors have a central
684 role in nitrate signalling." *Nature communications* 4: 1617. https://doi.org/10.1038/ncomms2621.
685
686 Krapp, A., R. Berthomé, M. Orsel, et al. 2011. "Arabidopsis roots and shoots show distinct
687 temporal adaptation patterns toward nitrogen starvation." *Plant Physiology* 157: 1255–1282.
688 https://doi.org/10.1104/pp.111.179838.
689
690 Krouk, G, B. Lacombe, A. Bielach, et al. 2010. "Nitrate-regulated auxin transport by NRT1.1
691 defines a mechanism for nutrient sensing in plants." *Developmental Cell* 18: 927–937.
692 https://doi.org/10.1016/j.devcel.2010.05.008.
693
694 Kuroha, T., H. Tokunaga, M. Kojima, et al. 2009. "Functional analyses of *LONELY GUY*
695 cytokinin-activating enzymes reveal the importance of the direct activation pathway in
696 *Arabidopsis*." *Plant Cell* 21: 3152–3169. https://doi.org/10.1105/tpc.109.068676.
697

698 Langmead, B., C. Trapnell, M. Pop, and S. L. Salzberg. 2009. "Ultrafast and memory-efficient
699 alignment of short DNA sequences to the human genome." *Genome Biology* 10: R25.
700 https://doi.org/10.1186/gb-2009-10-3-r25.
701
702 Laplaze, L., E. Benkova, I. Casimiro, et al. 2007. "Cytokinins act directly on lateral root founder
703 cells to inhibit root initiation." *Plant Cell* 19: 3889–3900. https://doi.org/10.1105/tpc.107.055863.
704
705 Léran, S., K. H. Edel, M. Pervent, et al. 2015. "Nitrate sensing and uptake in *Arabidopsis* are
706 enhanced by ABI2, a phosphatase inactivated by the stress hormone abscisic acid." *Science*
707 *Signaling* 8: ra43. DOI: 10.1126/scisignal.aaa4829.
708
709 Liu, K. H., C. Y. Huang, and Y. F. Tsay. 1999. "CHL1 is a dual-affinity nitrate transporter of
710 Arabidopsis involved in multiple phases of nitrate uptake." *Plant Cell* 11: 865–874.
711 https://doi.org/10.1105/tpc.11.5.865.
712
713 Liu, K. H., Y. Niu, M. Konishi, et al. 2017. "Discovery of nitrate–CPK–NLP signalling in central
714 nutrient–growth networks." *Nature* 545: 311–316. https://doi.org/10.1038/nature22077.
715
716 Liu, K. H., M. Liu, Z. Lin, et al. 2022. "NIN-like protein 7 transcription factor is a plant nitrate
717 sensor." *Science* 377: 1419–1425. https://doi.org/10.1126/science.add1104.
718
719 Maeda, Y., M. Konishi, T. Kiba, et al. 2018. "A NIGT1-centred transcriptional cascade regulates
720 nitrate signalling and incorporates phosphorus starvation signals in *Arabidopsis*." *Nature*
721 *Communications* 9: 1376. https://doi.org/10.1038/s41467-018-03832-6.
722

723 Marchive, C., F. Roudier, L. Castaings, et al. 2013. "Nuclear retention of the transcription factor
724 NLP7 orchestrates the early response to nitrate in plants." *Nature communications* 4: 1713.
725 https://doi.org/10.1038/ncomms2650.
726
727 Medici, A., and G. Krouk. 2014. "The primary nitrate response: a multifaceted signalling
728 pathway." *Journal of Experimental Botany* 65: 5567–5576. https://doi.org/10.1093/jxb/eru245.
729
730 Miyawaki, K., M. Matsumoto-Kitano, and T. Kakimoto. 2004. "Expression of cytokinin
731 biosynthetic isopentenyltransferase genes in *Arabidopsis*: tissue specificity and regulation by
732 auxin, cytokinin, and nitrate." *Plant Journal* 37: 128–138. https://doi.org/10.1046/j.1365-
733 313X.2003.01945.x.
734
735 Miyawaki, K., P. Tarkowski , M. Matsumoto-Kitano, et al. 2006. "Roles of *Arabidopsis*
736 ATP/ADP isopentenyltransferases and tRNA isopentenyltransferases in cytokinin biosynthesis."
737 *Proceedings of the National Academy of Sciences of the United States of America* 103: 16598–
738 16603. https://doi.org/10.1073/pnas.0603522103.
739
740 Monden, K., T. Kamiya, D. Sugiura, T. Suzuki, T. Nakagawa, and T. Hachiya. 2022. "Root-
741 specific activation of plasma membrane H^+-ATPase 1 enhances plant growth and shoot
742 accumulation of nutrient elements under nutrient-poor conditions in *Arabidopsis thaliana*."
743 *Biochemical and Biophysical Research Communications* 621: 39–45.
744 https://doi.org/10.1016/j.bbrc.2022.06.097.
745
746 Nacry, P., E. Bouguyon, and A. Gojon. 2013. "Nitrogen acquisition by roots: physiological and
747 developmental mechanisms ensuring plant adaptation to a fluctuating resource." *Plant and Soil*
748 370: 1–29. https://doi.org/10.1007/s11104-013-1645-9.

Ohkubo, Y., M. Tanaka, R. Tabata, M. Ogawa-Ohnishi, and Y. Matsubayashi. 2017. "Shoot-to-root mobile polypeptides involved in systemic regulation of nitrogen acquisition." *Nature Plants* 3: 17029. https://doi.org/10.1038/nplants.2017.29.

Okamoto, Y., T. Suzuki, D. Sugiura, T. Kiba, H. Sakakibara, and T. Hachiya. 2019. "Shoot nitrate underlies a perception of nitrogen satiety to trigger local and systemic signaling cascades in *Arabidopsis thaliana*." *Soil Science and Plant Nutrition* 65: 56–64. https://doi.org/10.1080/00380768.2018.1537643.

Osugi, A., M. Kojima, Y. Takebayashi, N. Ueda, T. Kiba, and H. Sakakibara. 2017. "Systemic transport of *trans*-zeatin and its precursor have differing roles in *Arabidopsis* shoots." *Nature Plants* 3: 17112. https://doi.org/10.1038/nplants.2017.112.

Ota, R., Y. Ohkubo, Y. Yamashita, M. Ogawa-Ohnishi, and Y. Matsubayashi. 2020. "Shoot-to-root mobile CEPD-like 2 integrates shoot nitrogen status to systemically regulate nitrate uptake in *Arabidopsis*." *Nature Communications* 11: 641. https://doi.org/10.1038/s41467-020-14440-8.

Patterson, K., L. A. Walters, A. M. Cooper, et al. 2016. "Nitrate-regulated glutaredoxins control Arabidopsis primary root growth." *Plant Physiology* 170: 989–999. https://doi.org/10.1104/pp.15.01776.

Poitout, A., A. Crabos, I. Petřík, et al. 2018. "Responses to systemic nitrogen signaling in Arabidopsis roots involve *trans*-zeatin in shoots." *Plant Cell* 30: 1243–1257. https://doi.org/10.1105/tpc.18.00011.

Remans, T., P. Nacry, M. Pervent, et al. 2006. "The *Arabidopsis* NRT1.1 transporter participates in the signaling pathway triggering root colonization of nitrate-rich patches." *Proceedings of the National Academy of Sciences of the United States of America* 103: 19206–19211. https://doi.org/10.1073/pnas.060527510.

Riveras, E., J. M. Alvarez, E. A. Vidal, C. Oses, A. Vega, and R. A. Gutiérrez. 2015. "The calcium ion is a second messenger in the nitrate signaling pathway of Arabidopsis." *Plant Physiology* 169: 1397–1404. https://doi.org/10.1104/pp.15.00961.

Rubin, G., T. Tohge, F. Matsuda, K. Saito, and W. R. Scheible. 2009. "Members of the *LBD* family of transcription factors repress anthocyanin synthesis and affect additional nitrogen responses in *Arabidopsis*." *Plant Cell* 21: 3567–3584. https://doi.org/10.1105/tpc.109.067041.

Ruffel, S., G. Krouk, D. Ristova, D. Shasha, K. D. Birnbaum, and G. M. Coruzzi. 2011. "Nitrogen economics of root foraging: transitive closure of the nitrate–cytokinin relay and distinct systemic signaling for N supply vs. demand." *Proceedings of the National Academy of Sciences of the United States of America* 108: 18524–18529. https://doi.org/10.1073/pnas.1108684108.

Sakakibara, H., K. Takei, and N. Hirose. 2006. "Interactions between nitrogen and cytokinin in the regulation of metabolism and development." *Trends in Plant Science* 11: 440–448. https://doi.org/10.1016/j.tplants.2006.07.004.

Sakakibara, H. 2021. "Cytokinin biosynthesis and transport for systemic nitrogen signaling." *Plant Journal* 105: 421–430. https://doi.org/10.1111/tpj.15011.

800 Safi, A., A. Medici, W. Szponarski, et al. 2021. "GARP transcription factors repress Arabidopsis
801 nitrogen starvation response via ROS-dependent and -independent pathways." *Journal of*
802 *Experimental Botany* 72: 3881–3901. https://doi.org/10.3390/ijms22168685.
803
804 Scheible, W. R., M. Lauerer, E. D. Schulze, M. Caboche, and M. Stitt. 1997. "Accumulation of
805 nitrate in the shoot acts as a signal to regulate shoot-root allocation in tobacco." *Plant Journal* 11:
806 671–691. https://doi.org/10.1046/j.1365-313X.1997.11040671.x.
807
808 Signora, L., I. De Smet, C. H. Foyer, and H. Zhang. 2001. "ABA plays a central role in mediating
809 the regulatory effects of nitrate on root branching in *Arabidopsis*." *Plant Journal* 28: 655–662.
810 https://doi.org/10.1046/j.1365-313x.2001.01185.x.
811
812 Su, H., T. Wang, C. Ju, et al. 2021. "Abscisic acid signaling negatively regulates nitrate uptake
813 via phosphorylation of NRT1. 1 by SnRK2s in *Arabidopsis*." *Journal of Integrative Plant Biology*
814 63: 597–610. https://doi.org/10.1111/jipb.13057.
815
816 Tabata, R., K. Sumida, T. Yoshii, K. Ohyama, H. Shinohara, and Y. Matsubayashi. 2014.
817 "Perception of root-derived peptides by shoot LRR-RKs mediates systemic N-demand signaling."
818 *Science* 346: 343–346. DOI: 10.1126/science.1257800.
819
820 Takei, K., N. Ueda, K. Aoki, et al. 2004a. "*AtIPT3* is a key determinant of nitrate-dependent
821 cytokinin biosynthesis in *Arabidopsis*." *Plant & Cell Physiology* 45: 1053–1062.
822 https://doi.org/10.1093/pcp/pch119.
823

824 Takei, K., T. Yamaya, and H. Sakakibara. 2004b. "Arabidopsis *CYP735A1* and *CYP735A2*
825 encode cytokinin hydroxylases that catalyze the biosynthesis of *trans*-zeatin." *Journal of*
826 *Biological Chemistry* 279: 41866–41872. https://doi.org/10.1074/jbc.M406337200.
827
828 Tokunaga, H., M. Kojima, T. Kuroha, et al. 2011. "Arabidopsis lonely guy (LOG) multiple
829 mutants reveal a central role of the LOG-dependent pathway in cytokinin activation." *Plant*
830 *Journal* 69: 355–365. https://doi.org/10.1111/j.1365-313X.2011.04795.x.
831
832 Wang, R., R. Tischner, R. A. Gutiérrez, et al. 2004. "Genomic analysis of the nitrate response
833 using a nitrate reductase-null mutant of Arabidopsis." *Plant Physiology* 136: 2512–2522.
834 https://doi.org/10.1104/pp.104.044610.
835
836 Wang, R, X. Xing, and N. M. Crawford. 2007. "Nitrite acts as a transcriptome signal at
837 micromolar concentrations in Arabidopsis roots." *Plant Physiology* 145: 1735–1745.
838 https://doi.org/10.1104/pp.107.108944.
839
840 Wang, X., C. Feng, L. Tian, et al. 2021. "A transceptor–channel complex couples nitrate sensing
841 to calcium signaling in *Arabidopsis*." *Molecular Plant* 14: 774–786.
842 https://doi.org/10.1016/j.molp.2021.02.005.
843
844 Wang, H., C. Han, J. G. Wang, et al. 2022. "Regulatory functions of cellular energy sensor SnRK1
845 for nitrate signalling through NLP7 repression." *Nature Plants* 8: 1094-1107.
846 https://doi.org/10.1038/s41477-022-01236-5.
847
848 Werner, T., V. Motyka, V. Laucou, R. Smets, H. Van Onckelen, and T. Schmülling. 2003.
849 "Cytokinin-deficient transgenic Arabidopsis plants show multiple developmental alterations

850 indicating opposite functions of cytokinins in the regulation of shoot and root meristem activity."
851 *Plant Cell* 15: 2532–2550. https://doi.org/10.1105/tpc.014928.
852
853 Werner, T., K. Holst, Y. Pörs, et al. 2008. "Cytokinin deficiency causes distinct changes of sink
854 and source parameters in tobacco shoots and roots." *Journal of Experimental Botany* 59: 2659–
855 2672. https://doi.org/10.1093/jxb/ern134.
856
857 Wu, B., J. Meng, H. Liu, et al. 2023. "Suppressing a phosphohydrolase of cytokinin nucleotide
858 enhances grain yield in rice." *Nature Genetics* 55: 1381–1389. https://doi.org/10.1038/s41588-
859 023-01454-3.
860
861 Xu, N., R. Wang, L. Zhao, et al. 2016. "The Arabidopsis NRG2 protein mediates nitrate signaling
862 and interacts with and regulates key nitrate regulators." *Plant Cell* 28: 485–504.
863 https://doi.org/10.1105/tpc.15.00567.
864
865 Zhou, Y., B. Zhou, L. Pache, et al. 2019. "Metascape provides a biologist-oriented resource for
866 the analysis of systems-level datasets." *Nature Communications* 10: 1523.
867 https://doi.org/10.1038/s41467-019-09234-6.
868
869 Zhang, H., A. Jennings, P. W. Barlow, and B. G. Forde. 1999. "Dual pathways for regulation of
870 root branching by nitrate." *Proceedings of the National Academy of Sciences of the United States*
871 *of America* 96: 6529–6534. https://doi.org/10.1073/pnas.96.11.6529.
872
873 Zhang, K., O. Novak, Z. Wei, et al. 2014. "*Arabidopsis* ABCG14 protein controls the acropetal
874 translocation of root-synthesized cytokinins." *Nature Communications* 5: 3274.
875 https://doi.org/10.1038/ncomms4274.

876

877 **Supporting Information**

878 Additional supporting information can be found online in the Supporting Information section.

879

880 **Figure Legends**

881 **Figure 1.** Micrografting and transfer experiments for manipulation of nitrate levels and *IPT3*
882 expression in a shoot-specific manner. (A) Summary of the micrografting and transfer
883 experiments. (B) A schematic representation of four types of grafted plants. The dotted line
884 represents the grafted seam in the hypocotyl. (C, D) Nitrate concentrations in shoots (C) and roots
885 (D) 0, 3, or 5 days after nitrogen removal. (E, F) Total protein concentrations in shoots (E) and
886 roots (F) 5 days after nitrogen removal. (C–F) Two grafted plants were pooled as one biological
887 replicate. Data are presented as mean ± SD (n = 3). (G, H) Total nitrogen concentrations in shoots
888 (G) and roots (H) 5 days after nitrogen removal. Sampling was performed three times
889 independently. In this sampling, 7, 6, and 5 grafted plants were pooled as one biological replicate.
890 Data are presented as mean ± SD (n = 3). (C–H) Different lowercase letters indicate significant
891 differences, as determined via Tukey–Kramer test ($P < 0.05$). (I) Transcript levels of *IPT3* in
892 shoots 5 days after nitrogen removal, as determined using RT-qPCR. Sampling was done five
893 times independently. In this sampling, 9, 6, 7, 7, and 8 grafted plants were pooled as one biological
894 replicate. Data are presented as mean ± SD (n = 5). (J) Nitrate concentrations in shoots 5 days
895 after nitrogen removal. (K) Transcript levels of *GFP* in shoots 5 days after nitrogen removal, as
896 determined via RT-qPCR. (J, K) One biological replicate consisted of one grafted plant. Data are
897 presented as mean ± SD (n = 3). (I–K) Statistical significance was assessed using unpaired two-
898 tailed Welch's *t*-test (*$P < 0.05$; **$P < 0.01$; ***$P < 0.001$). (L) Fluorescence images of true
899 leaves 5 days after nitrogen removal. Green and red colors correspond to GFP fluorescence and
900 autofluorescence, respectively. Scale bars represent 500 μm. In graph legends, the grafted plants

901 are indicated as "scion line name/rootstock line name." ns, not significant; FW, fresh weight; DW,
902 dry weight.
903
904 **Figure 2.** Effects of shoot nitrate status and shoot *IPT3* expression on the shoot and root
905 concentrations of CK species. (A–M) The shoot and root concentrations of iP (A), iPR (B), iPRPs
906 (C), iP7G (D), iP9G (E), *t*Z (F), *t*ZR (G), *t*ZPRs (H), *t*Z7G (I), *t*Z9G (J), *t*ZOG (K), *t*ZROG (L),
907 and *t*ZRPsOG (M) in the grafted plants 5 days after nitrogen removal (condition 5). Sampling
908 was performed three times independently. In the sampling, 7, 6, and 5 grafted plants were pooled
909 as one biological replicate. Data are presented as mean ± SD [n = 3, excluding iP concentrations
910 in Col/*ipt3,5,7* roots and *ipt3*/*ipt3,5,7* roots (n = 2)]. Different lowercase letters indicate
911 significant differences, as determined via Tukey–Kramer test ($P < 0.05$). Regarding the shoot
912 concentrations of iP and *t*ZRPsOG, unpaired two-tailed Welch's *t*-test was run at $\alpha = 0.05$. iP, N^6-
913 (Δ^2-isopentenyl)adenine; iPR, iP riboside; iPRPs, iP ribotides; iP7G, iP-7-*N*-glucoside; iP9G, iP-
914 9-*N*-glucoside; *t*Z, *trans*-zeatin; *t*ZR, *t*Z riboside; *t*ZRPs, *t*Z ribotides; *t*Z7G, *t*Z-7-*N*-glucoside;
915 *t*Z9G, *t*Z-9-*N*-glucoside; *t*ZOG, *t*Z-*O*-glucoside; *t*ZROG, *t*ZR-*O*-glucoside; *t*ZRPsOG, *t*ZRPs-*O*-
916 glucoside; ns, not significant; nd, not detected; FW, fresh weight.
917
918 **Figure 3.** Effects of shoot nitrate status and shoot *IPT3* expression on plant growth. (A)
919 Representative shoot appearance of grafted plants. Scale bars represent 5 mm. (B–F) Shoot fresh
920 weight (B), leaf blade area (C), rosette diameter (D), leaf number (E), root fresh weights (F), and
921 fresh weight ratios of shoot to root (G) of grafted plants 5 days after nitrogen removal (condition
922 5). All data pooled from five independent grafting experiments are presented as mean ± SD (n =
923 33). Different lowercase letters indicate significant differences, as determined via Tukey–Kramer
924 test ($P < 0.05$). ns, not significant; FW, fresh weight.
925
926 **Figure 4.** Effects of shoot nitrate status and shoot *IPT3* expression on the shoot and root

927 transcriptomes. RNA-seq was performed using the shoots and roots of grafted plants 5 days after
928 nitrogen removal (condition 5). Sampling was performed three times independently. In the
929 sampling, 9, 6, and 7 grafted plants were pooled as one biological replicate. (A) Venn diagram
930 presenting the number of DEGs at a minimum fold change of 1.5 in NR-null/*ipt3,5,7* plants
931 relative to Col/*ipt3,5,7* plants and in NR-null *ipt3*/*ipt3,5,7* plants relative to *ipt3*/*ipt3,5,7* plants.
932 (B–E) Plots of normalized transcript levels of 631 DEGs (B) and 663 DEGs (C) in shoots and
933 189 DEGs (D) and 126 DEGs (E) in roots. 1st, 2nd, and 3rd denote the order of three independent
934 experiments. Different lowercase letters indicate significant differences, as determined via
935 Tukey–Kramer test ($P < 0.05$). The numbers on the graph represent the difference in mean values.
936
937 **Figure 5.** Effects of shoot nitrate status and shoot *IPT3* expression on nitrogen-related
938 transcriptional responses in shoots and roots. (A–D) Plots of mean normalized transcript levels of
939 nitrate (*per se*)-inducible genes in 2 h (A), genes induced via CPK10/30/32 (B), genes commonly
940 induced via all NLPs (C), and nitrogen starvation-inducible genes (D) in the shoots and roots of
941 grafted plants 5 days after nitrogen removal (condition 5). The gene lists were obtained from
942 Wang et al. (2004) for (A), Liu et al. (2017) for (B), Liu et al. (2022) for (C), and Kiba et al.
943 (2018) and Krapp et al. (2011) for (D). Different lowercase letters indicate significant differences,
944 as determined via Tukey–Kramer test ($P < 0.05$). The numbers on the graph represent the
945 difference in mean values. (E–G) Transcriptional changes in genes involved in nitrogen transport
946 and assimilation in roots (E), genes encoding transcription factors for nitrogen starvation
947 responses in shoots (F) and in roots (G), and genes encoding shoot-to-root mobile peptides in
948 shoots (H) in grafted plants 5 days after nitrogen removal. The normalized transcript levels were
949 visualized as heatmaps using MORPHEUS (https://software.broadinstitute.org/morpheus). The
950 relative color scheme uses the minimum (blue) and maximum (yellow) values in each row. 1st,
951 2nd, and 3rd denote the order of three independent experiments. ns, not significant; TF,
952 transcription factor.

953

954 **Figure 6.** Summary of systemic responses to shoot nitrate accumulation and their dependence by

955 shoot IPT3.

Figure 1

(A) Procedure for transfer experiment

	Condition 1 →	Condition 2 →	Condition 3 →	Condition 4 →	Condition 5
Duration	4 days	5 days	24 hours	24 hours	0, 3, 5 days
N source	2.5 mM NH_4^+	2.5 mM NH_4^+	2.5 mM NH_4^+	10 mM NO_3^- & 2.5 mM NH_4^+	No nitrogen
pH	6.7	6.7	6.7	6.7	5.7
PPFD	25 μmol m^{-2} s^{-1}	50 μmol m^{-2} s^{-1}	25 μmol m^{-2} s^{-1}	25 μmol m^{-2} s^{-1}	25 μmol m^{-2} s^{-1}
Temperature	22°C	27°C	22°C	22°C	22°C

▲ Micrografting ▲ NO_3^- supply ▲ Nitrogen removal

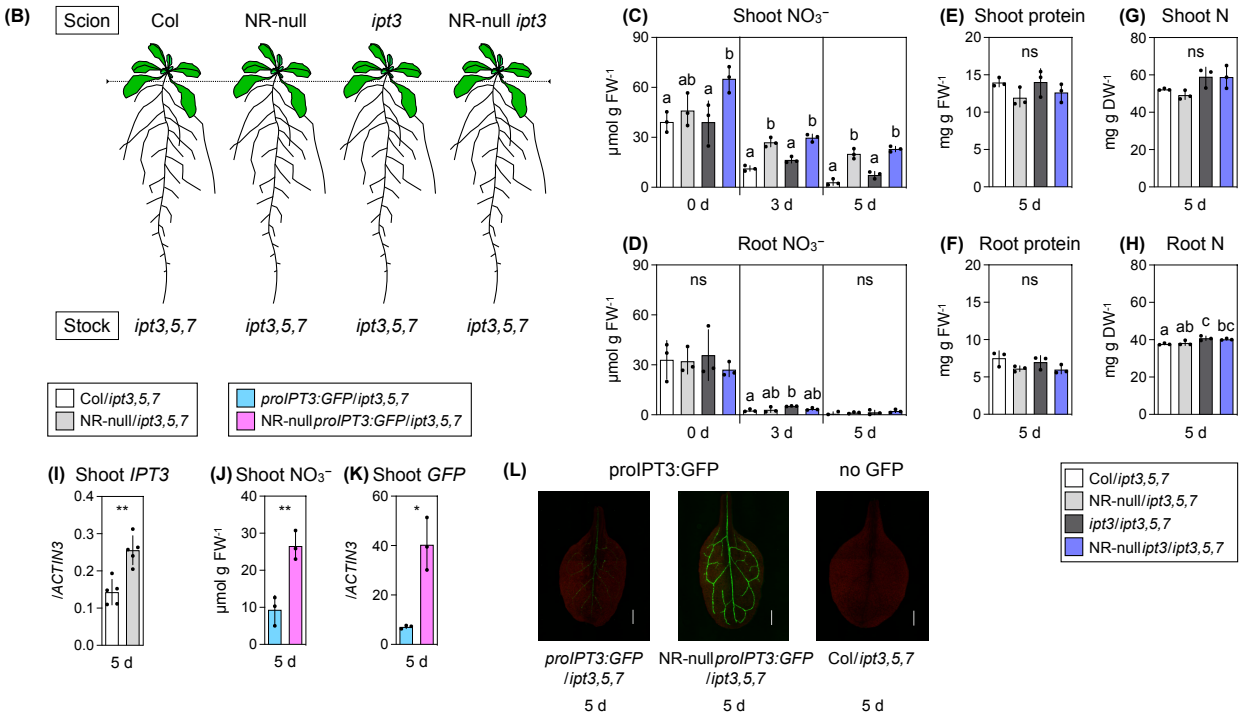

Figure 1. Micrografting and transfer experiments for manipulation of nitrate levels and *IPT3* expression in a shoot-specific manner. (A) Summary of the micrografting and transfer experiments. (B) A schematic representation of four types of grafted plants. The dotted line represents the grafted seam in the hypocotyl. (C, D) Nitrate concentrations in shoots (C) and roots (D) 0, 3, or 5 days after nitrogen removal. (E, F) Total protein concentrations in shoots (E) and roots (F) 5 days after nitrogen removal. (C–F) Two grafted plants were pooled as one biological replicate. Data are presented as mean ± SD (n = 3). (G, H) Total nitrogen concentrations in shoots (G) and roots (H) 5 days after nitrogen removal. Sampling was performed three times independently. In this sampling, 7, 6, and 5 grafted plants were pooled as one biological replicate. Data are presented as mean ± SD (n = 3). (C–H) Different lowercase letters indicate significant differences, as determined via Tukey–Kramer test ($P < 0.05$). (I) Transcript levels of *IPT3* in shoots 5 days after nitrogen removal, as determined using RT-qPCR. Sampling was done five times independently. In this sampling, 9, 6, 7, 7, and 8 grafted plants were pooled as one biological replicate. Data are presented as mean ± SD (n = 5). (J) Nitrate concentrations in shoots 5 days after nitrogen removal. (K) Transcript levels of *GFP* in shoots 5 days after nitrogen removal, as determined via RT-qPCR. (J, K) One biological replicate consisted of one grafted plant. Data are presented as mean ± SD (n = 3). (I–K) Statistical significance was assessed using unpaired two-tailed Welch's *t*-test (*$P < 0.05$; **$P < 0.01$; ***$P < 0.001$). (L) Fluorescence images of true leaves 5 days after nitrogen removal. Green and red colors correspond to GFP fluorescence and autofluorescence, respectively. Scale bars represent 500 μm. In graph legends, the grafted plants are indicated as "scion line name/rootstock line name." ns, not significant; FW, fresh weight; DW, dry weight.

Figure 2

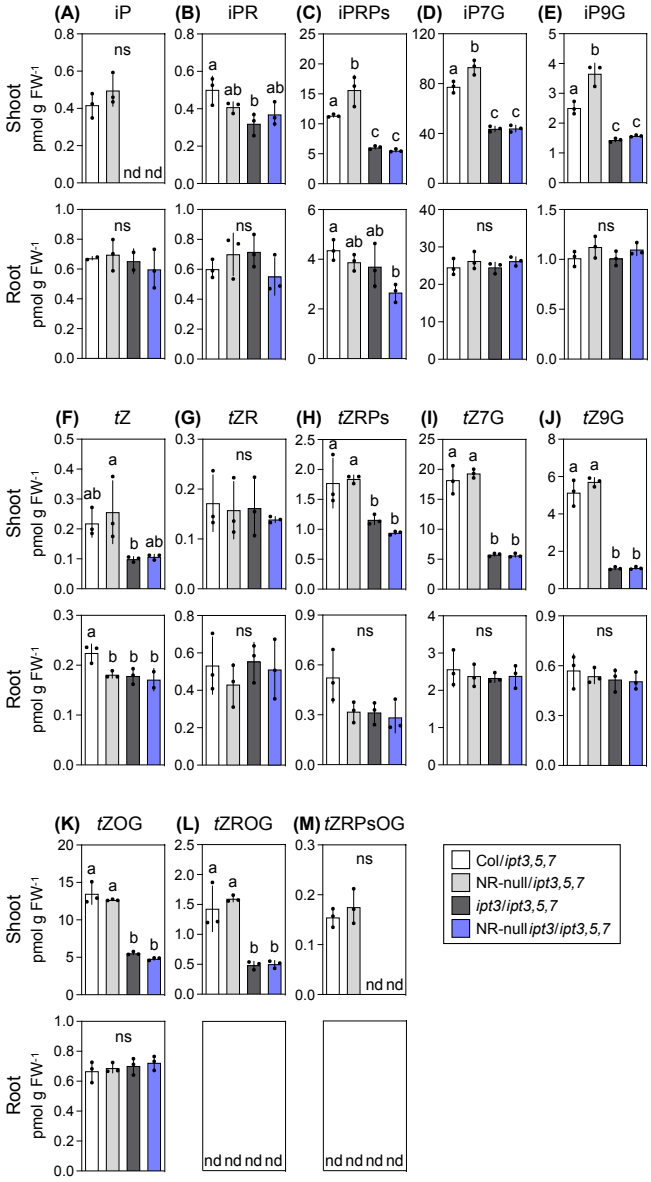

Figure 2. Effects of the shoot nitrate status and shoot *IPT3* expression on the shoot and root concentrations of CK species. (A–M) The shoot and root concentrations of iP (A), iPR (B), iPRPs (C), iP7G (D), iP9G (E), *t*Z (F), *t*ZR (G), *t*ZPRs (H), *t*Z7G (I), *t*Z9G (J), *t*ZOG (K), *t*ZROG (L), and *t*ZRPsOG (M) in the grafted plants 5 days after nitrogen removal (condition 5). Sampling was performed three times independently. In the sampling, 7, 6, and 5 grafted plants were pooled as one biological replicate. Data are presented as mean ± SD [n = 3, excluding iP concentrations in Col/*ipt3,5,7* roots and *ipt3*/*ipt3,5,7* roots (n = 2)]. Different lowercase letters indicate significant differences, as determined via Tukey–Kramer test (P < 0.05). Regarding the shoot concentrations of iP and *t*ZRPsOG, unpaired two-tailed Welch's *t*-test was run at α = 0.05. iP, N^6-(Δ^2-isopentenyl)adenine; iPR, iP riboside; iPRPs, iP ribotides; iP7G, iP-7-*N*-glucoside; iP9G, iP-9-*N*-glucoside; *t*Z, *trans*-zeatin; *t*ZR, *t*Z riboside; *t*ZRPs, *t*Z ribotides; *t*Z7G, *t*Z-7-*N*-glucoside; *t*Z9G, *t*Z-9-*N*-glucoside; *t*ZOG, *t*Z-*O*-glucoside; *t*ZROG, *t*ZR-*O*-glucoside; *t*ZRPsOG, *t*ZRPs-*O*-glucoside; ns, not significant; nd, not detected; FW, fresh weight.

Figure 3

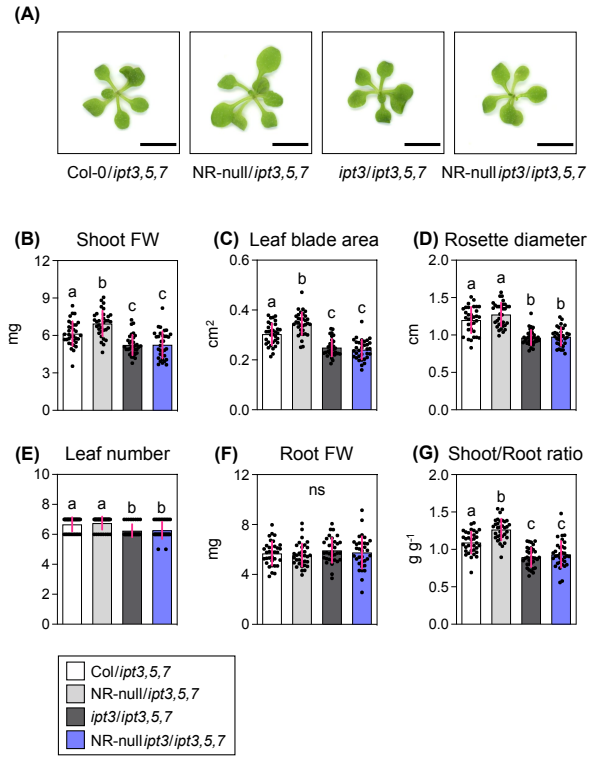

Figure 3. Effects of the shoot nitrate status and shoot *IPT3* expression on plant growth. (A) Representative shoot appearance of grafted plants. Scale bars represent 5 mm. (B–F) Shoot fresh weights (B), leaf blade area (C), rosette diameter (D), leaf number (E), root fresh weights (F), and fresh weight ratios of shoot to root (G) of grafted plants 5 days after nitrogen removal (condition 5). All data pooled from five independent grafting experiments are presented as mean ± SD (n = 33). Different lowercase letters indicate significant differences, as determined via Tukey–Kramer test ($P < 0.05$). ns, not significant; FW, fresh weight.

Figure 4

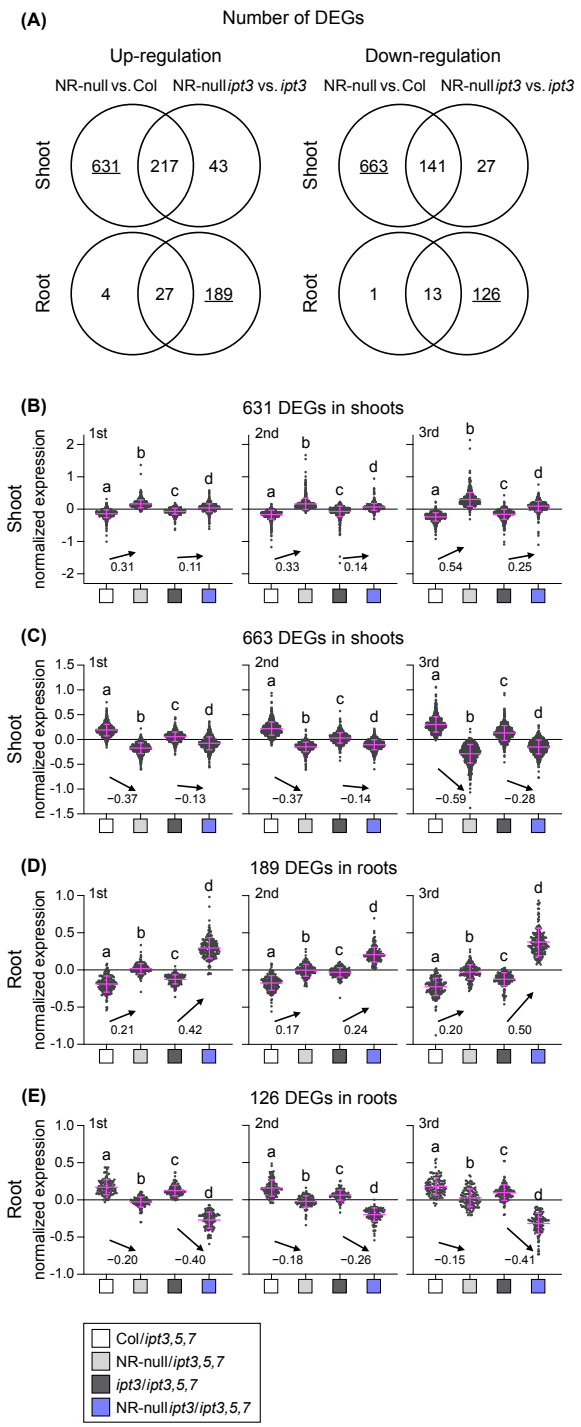

Figure 4. Effects of the shoot nitrate status and shoot *IPT3* expression on the shoot and root transcriptomes. RNA-seq was performed using the shoots and roots of grafted plants 5 days after nitrogen removal (condition 5). Sampling was performed three times independently. In the sampling, 9, 6, and 7 grafted plants were pooled as one biological replicate. (A) Venn diagram presenting the number of DEGs at a minimum fold change of 1.5 in NR-null/*ipt3,5,7* plants relative to Col/*ipt3,5,7* plants and in NR-null *ipt3*/*ipt3,5,7* plants relative to *ipt3*/*ipt3,5,7* plants. (B–E) Plots of normalized transcript levels of 631 DEGs (B) and 663 DEGs (C) in shoots and 189 DEGs (D) and 126 DEGs (E) in roots. 1st, 2nd, and 3rd denote the order of three independent experiments. Different lowercase letters indicate significant differences, as determined via Tukey–Kramer test ($P < 0.05$). The numbers on the graph represent the difference in mean values.

Figure 5

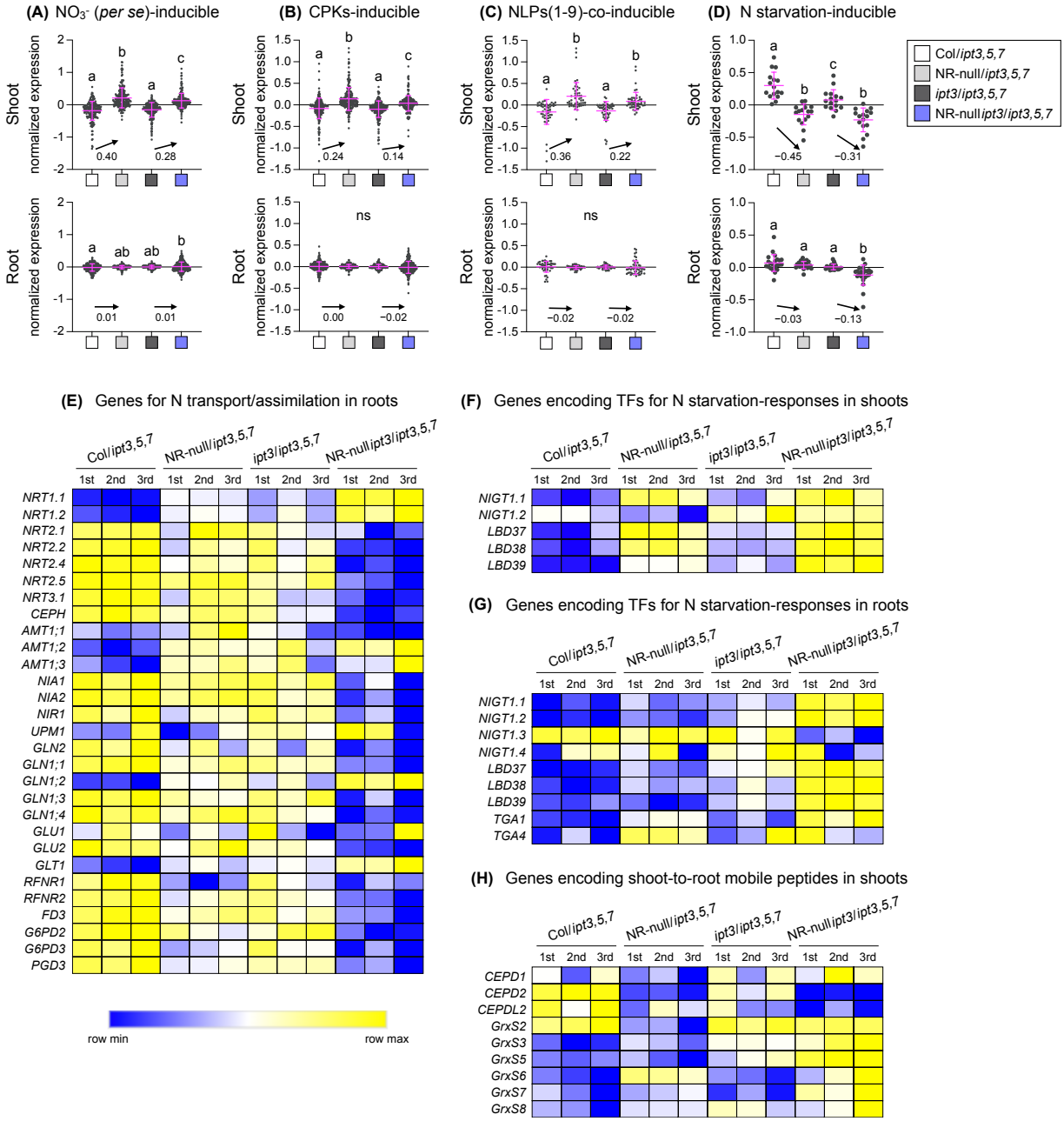

Figure 5. Effects of the shoot nitrate status and shoot *IPT3* expression on nitrogen-related transcriptional responses in shoots and roots. (A–D) Plots of mean normalized transcript levels of nitrate (*per se*)-inducible genes in 2 h (A), genes induced via CPK10/30/32 (B), genes commonly induced via all NLPs (C), and nitrogen starvation-inducible genes (D) in the shoots and roots of grafted plants 5 days after nitrogen removal (condition 5). The gene lists were obtained from Wang et al. (2004) for (A), Liu et al. (2017) for (B), Liu et al. (2022) for (C), and Kiba et al. (2018) and Krapp et al. (2011) for (D). Different lowercase letters indicate significant differences, as determined via Tukey–Kramer test ($P < 0.05$). The numbers on the graph represent the difference in mean values. (E–G) Transcriptional changes in genes involved in nitrogen transport and assimilation in roots (E), genes encoding transcription factors for nitrogen starvation responses in shoots (F) and in roots (G), and genes encoding shoot-to-root mobile peptides in shoots (H) in grafted plants 5 days after nitrogen removal. The normalized transcript levels were visualized as heatmaps using MORPHEUS (https://software.broadinstitute.org/morpheus). The relative color scheme uses the minimum (blue) and maximum (yellow) values in each row. 1st, 2nd, and 3rd denote the order of three independent experiments. ns, not significant; TF, transcription factor.

Figure 6

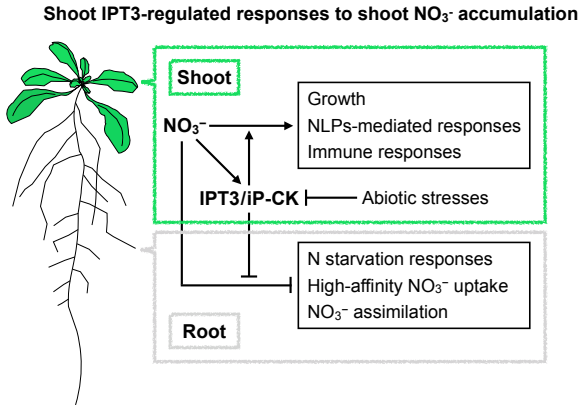

Figure 6. Summary of systemic responses to shoot nitrate accumulation and their modulation by shoot IPT3.